ADVANCED FUNCTIONAL MATERIALS

# Supporting Information

for *Adv. Funct. Mater.*, DOI: 10.1002/adfm.202008054

# Copper@ZIF-8 Core-Shell Nanowires for Reusable Antimicrobial Face Masks

*Abhishek Kumar, Anu Sharma, Yi Chen, Megan M. Jones, Stephen T. Vanyo, Changning Li, Michelle B. Visser, Supriya D. Mahajan, Rakesh Kumar Sharma,* and Mark T. Swihart**

**Supporting Information File**

**for**

# Copper@ZIF-8 core-shell nanowires for reusable antimicrobial face masks

*Abhishek Kumar[a#], Anu Sharma[a,b#], Yi Chen[a], Megan M Jones[c], Stephen T Vanyo[c], Changning Li[d], Michelle B Visser[c], Supriya D. Mahajan[e], Rakesh Kumar Sharma[b*], Mark T Swihart[a,f*]*

[a] Department of Chemical and Biological Engineering, University at Buffalo (SUNY), USA

[b] Department of Chemistry, University of Delhi, India

[c] Department of Oral Biology, University at Buffalo (SUNY), USA

[d] Department of Biomedical Engineering, University at Buffalo (SUNY), USA

[e] Department of Medicine, Division of Allergy, Immunology and Rheumatology, Jacobs School of Medicine and Biomedical Sciences, University at Buffalo (SUNY), USA

[f] RENEW Institute, University at Buffalo (SUNY), USA

[#] AK and AS contributed equally.

**KEYWORDS**: COVID-19, Copper Nanowires, ZIF-8, Metal-Organic Frameworks, Antibacterial Activity

*Corresponding author: swihart@buffalo.edu (M.T.S), sharmark@chemistry.du.ac.in (R.K.S.)

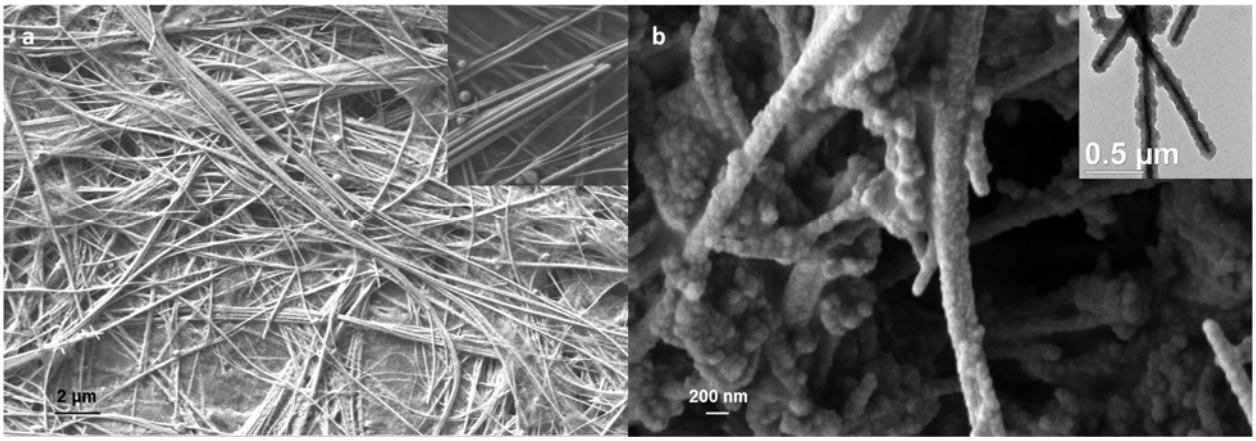


**Figure S1. (a)** SEM image of Cu NWs with larger diameter synthesized using less OAm; **(b)** SEM image of Cu@ZIF-8 nanowires with larger diameter.

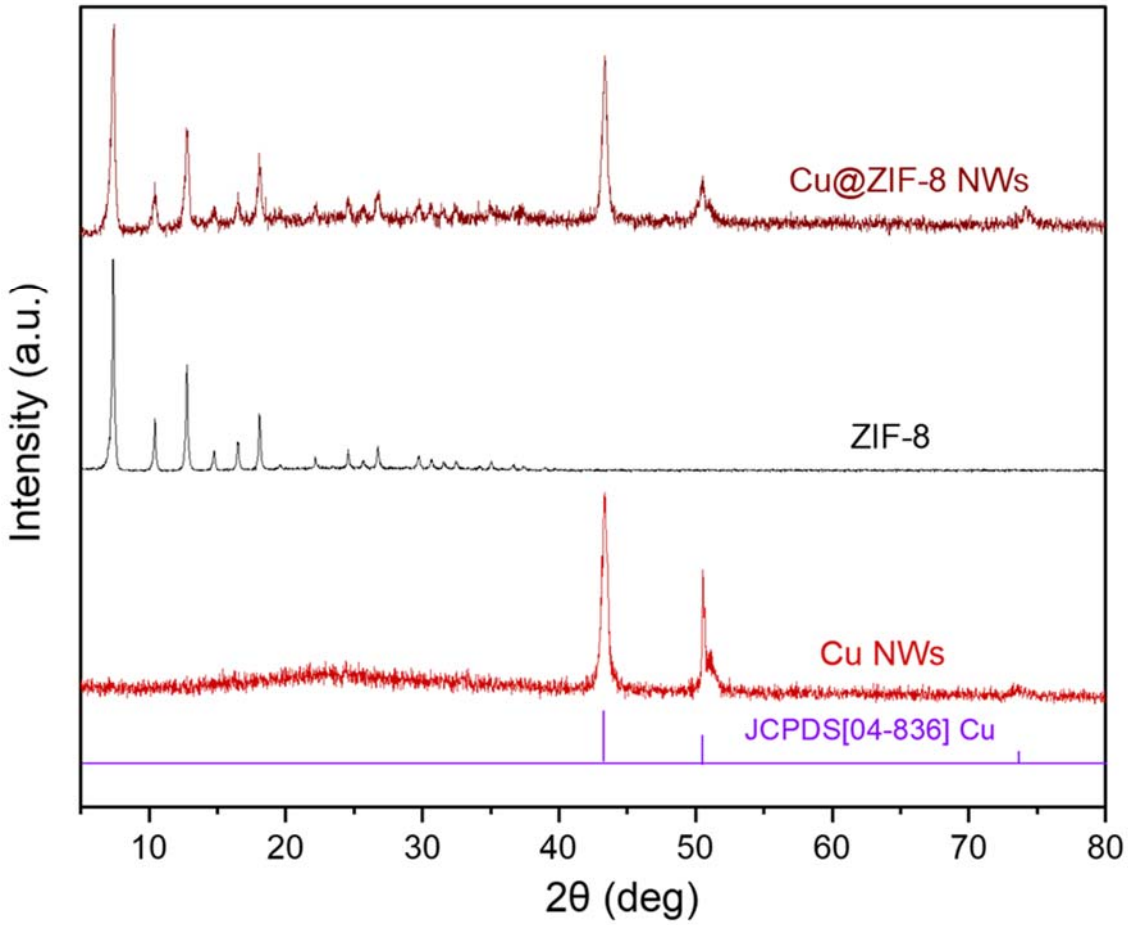


**Figure S2**. XRD patterns of Cu NWs, ZIF-8, and core shell Cu@ZIF-8 heterostructure NWs.

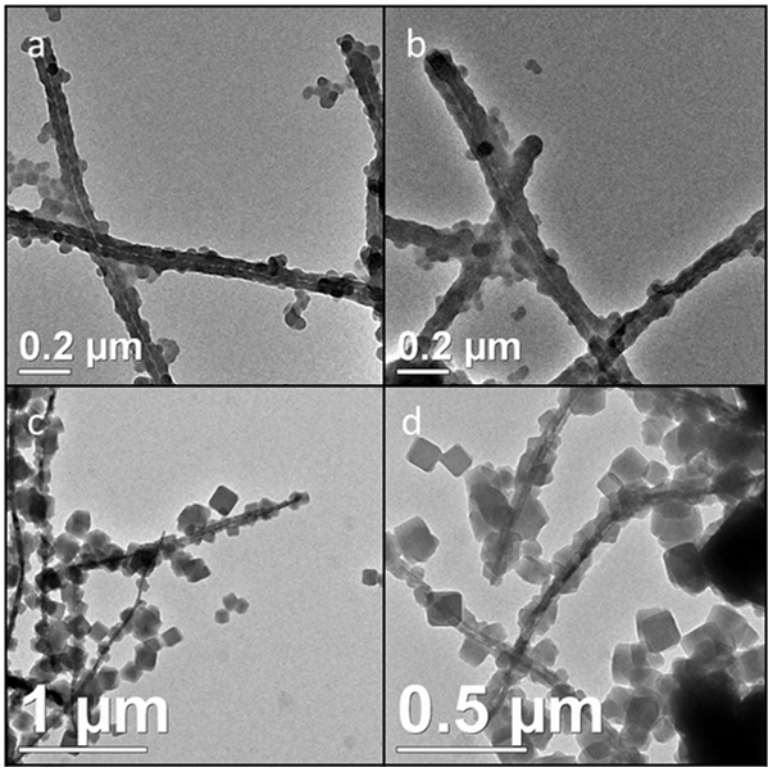


**Figure S3.** TEM images of **(a-b)** Hollow ZIF-8 nanotubes formed by attempts to synthesize Cu@ZIF-8 without PVP; **(c-d)** Cu@ZIF-8 NWs with PVP as surface passivating agent.

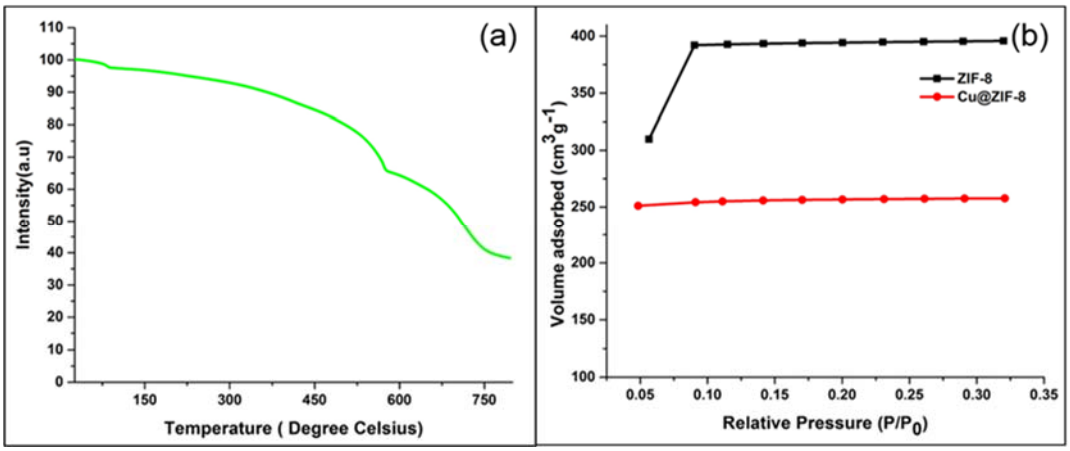


**Figure S4. (a)** TGA curve of Cu@ZIF-8 NWs **(b)** BET adsorption curve of ZIF-8, and core-shell Cu@ZIF-8 NWs respectively.

**Table S1.** Pore parameters of ZIF-8 and core-shell Cu@ZIF-8 NWs from BET and BJH analysis of nitrogen physisorption data.

| Sample | ZIF-8 | Cu@ZIF-8 NWs |
|---|---|---|
| $S_{BET}$ ($m^2/g$) | 893 | 583 |
| $S_{Lang}$($m^2/g$) | 1344 | 876 |
| Pore volume ($cm^3/g$) | 0.613 | 0.399 |
| Average pore width (nm) | 2.75 | 2.73 |

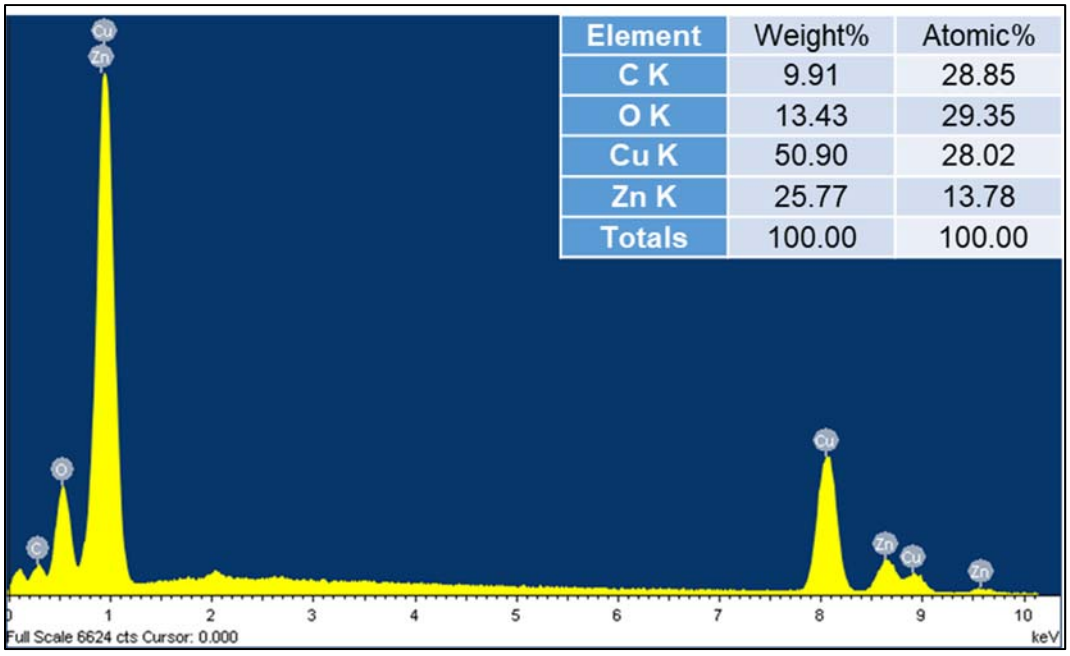


**Figure S5**. Representative EDS spectrum of Cu@ZIF-8 NWs with mean Cu:Zn ratio 2.09 and mean standard deviation of 0.17 from 3 measurements.

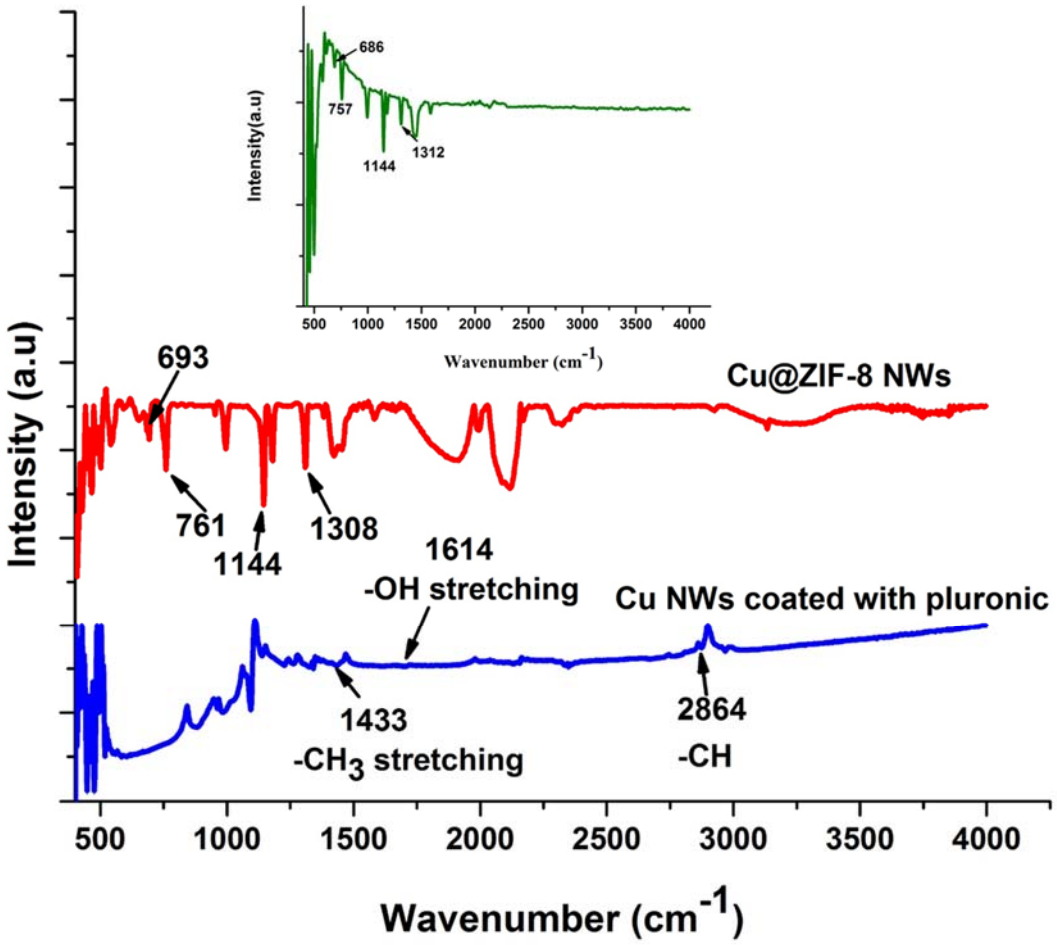


**Figure S6.** FTIR spectra of Cu NWs coated with pluronic and Cu@ZIF-8 NWs. Inset shows the FTIR spectrum of ZIF-8.

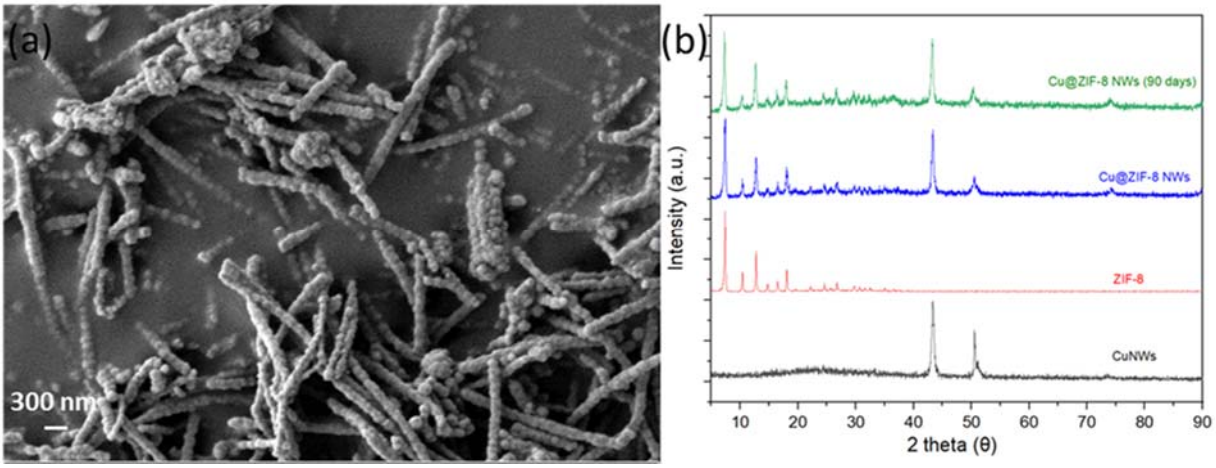


**Figure S7. (a)** SEM image of Cu@ZIF-8 NWs 90 days after synthesis; **(b)** XRD peaks for Cu@ZIF-8 NWs 90 days after synthesis, compared with that of freshly prepared Cu@ZIF-8 NWs

**Table S2: summary of filtration efficiency and corresponding differential pressure across different samples**

| Sample | 0.3 µm | 0.5 µm | 1.0 µm | 3.0 µm | 5.0 µm | 10.0 µm | Pressure Drop (in W.C.) @ 3 CFM | Pressure Drop (in W.C.) @ 1 CFM |
|---|---|---|---|---|---|---|---|---|
| N95 (REF) | 97.5% | 99.2% | 99.8% | 100.0% | 100.0% | 100.0% | 1.51 | 0.54 |
| S0 (untreated) | 72.2% | 86.1% | 95.3% | 97.5% | 100.0% | 100.0% | 0.82 | 0.29 |
| S1 (EtOH treated) | 38.1% | 56.2% | 77.4% | 100.0% | 100.0% | 100.0% | 0.64 | 0.22 |
| S2 (0.1 mg/ml) | 57.6% | 74.4% | 90.4% | 100.0% | 100.0% | 100.0% | 0.7 | 0.24 |
| S3 (0.25 mg/ml) | 70.0% | 82.9% | 94.0% | 100.0% | 100.0% | 100.0% | 0.69 | 0.24 |
| S4 (0.5 mg/ml)) | 80.2% | 89.7% | 95.2% | 100.0% | 100.0% | 100.0% | 0.85 | 0.3 |
| S5 (1 mg/ml) | 78.2% | 88.5% | 95.7% | 100.0% | 100.0% | 100.0% | 0.87 | 0.3 |

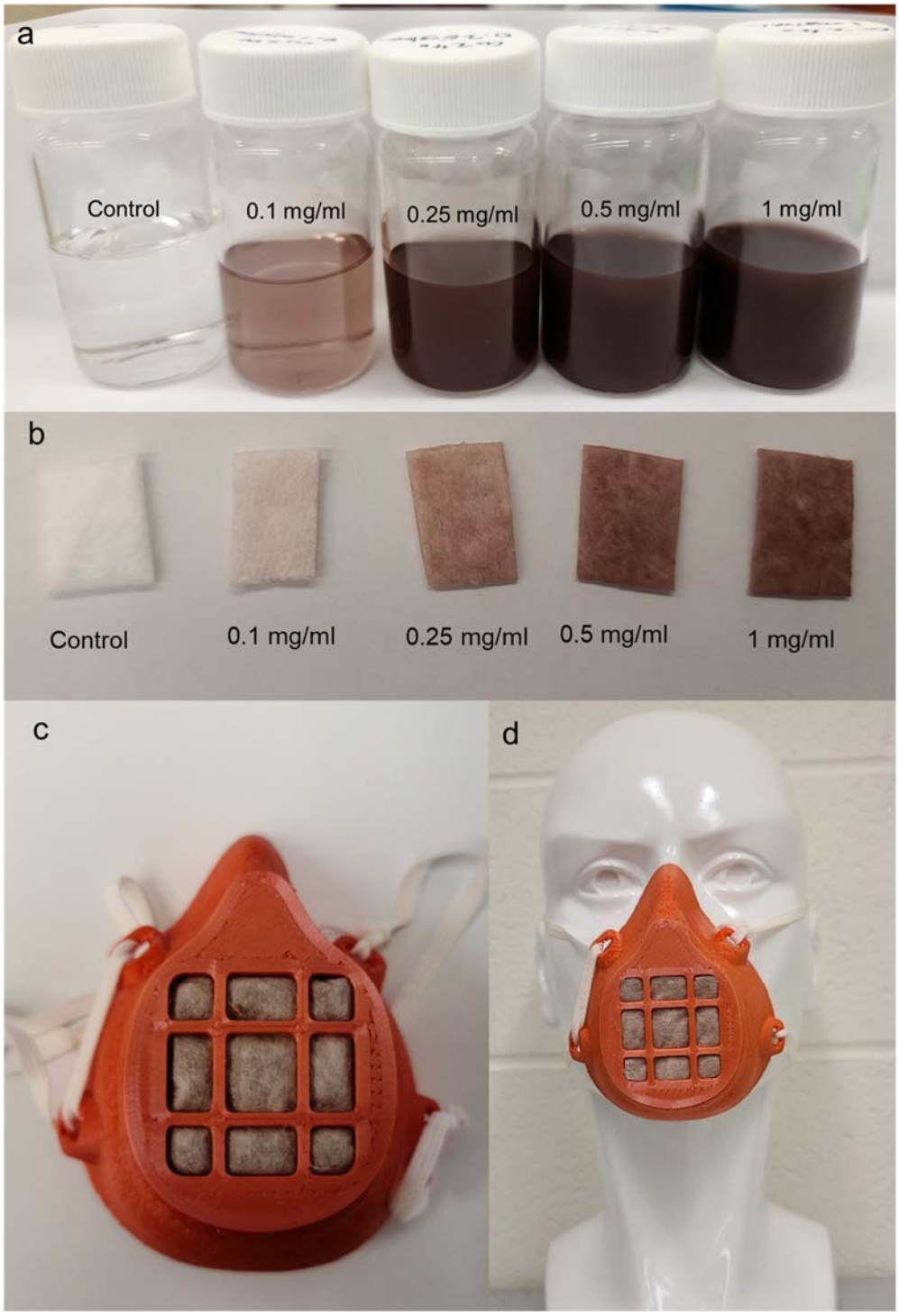


**Figure S8.** Photographs of **(a)** Cu@ZIF-8 NWs solution in ethanol, **(b)** filter media dipped in varying concentration of Cu@ZIIF-8 NWs, **(c)** filter media being used in a 3D printed facemask, **(d)** 3D printed facemask with Cu@ZIF-8 filter media on a mannequin head.

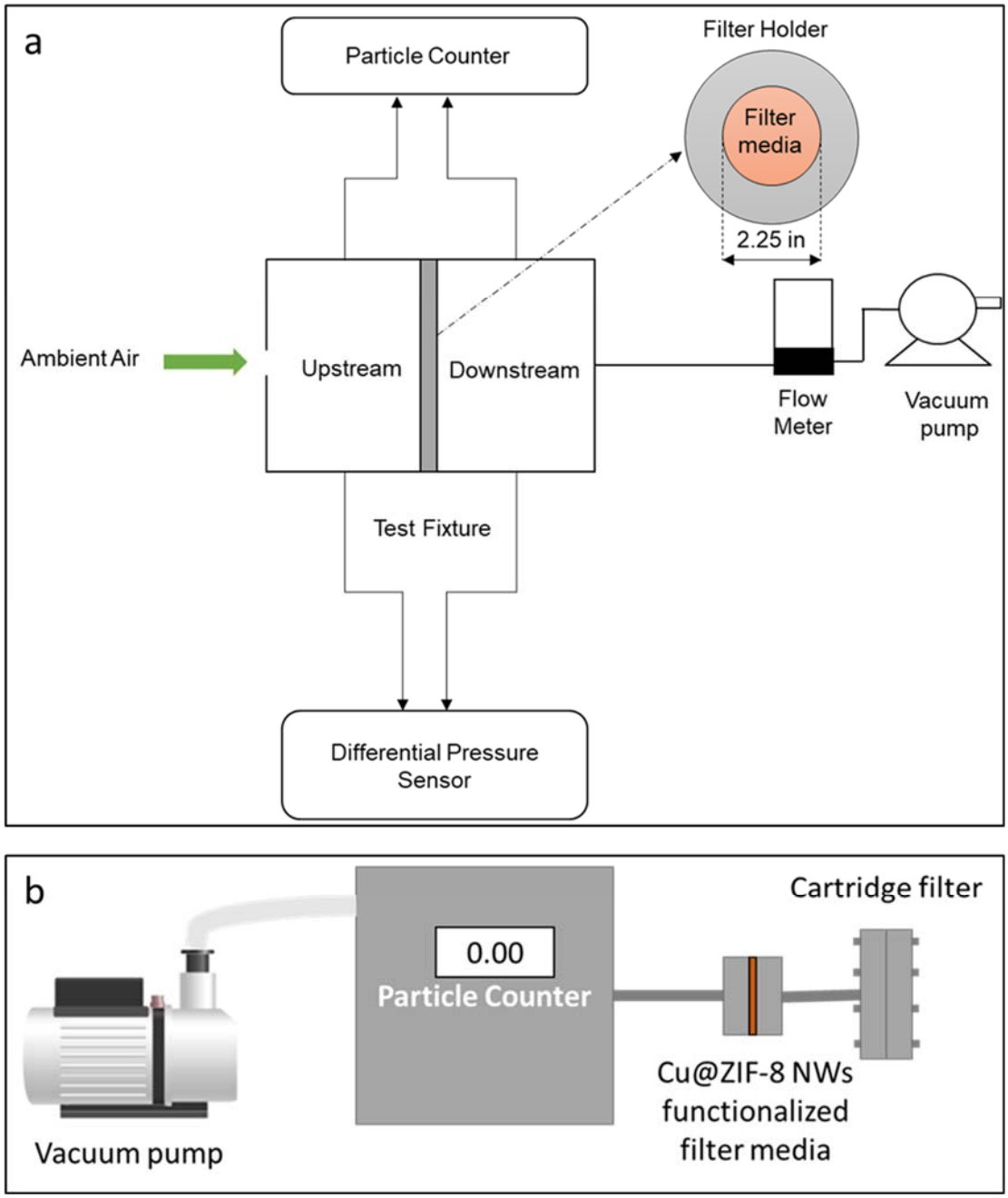


**Figure S9. (a)** Schematic of filtration efficiency measurements set-up. **(b)** Schematic of particle release study for Cu@ZIF-8 NWs functionalized filter media.

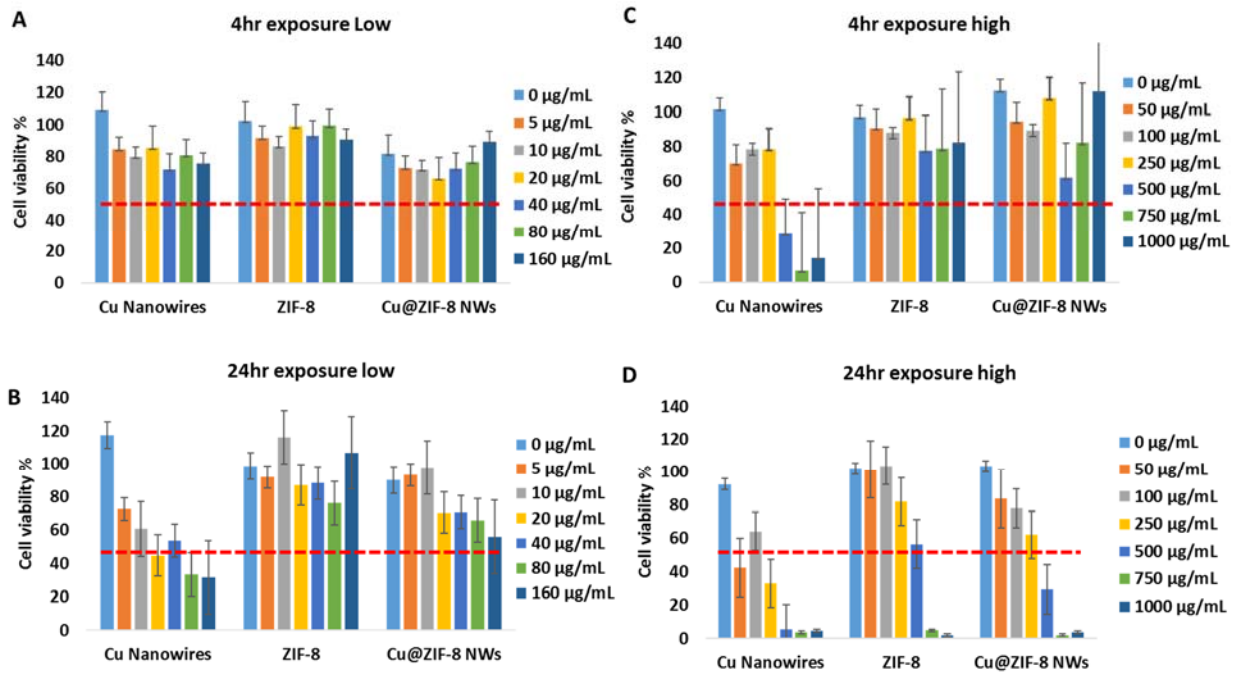


**Figure S10.** Effect of CuNWs, ZIF-8, and Cu@ZIF-8 NWs on viability of Human Gingival fibroblast cells using the MTT assay after 4 h and 24 h exposure. Our results show that Cu@ZIF-8 shows no significant decrease in cell viability up to 160 µg/mL for low dose exposure and up to 250 µg/mL for high dose exposures. Uncoated Cu NWs showed significant toxicity at levels $\geq$ 50 µg/mL. Data shown are mean ± SD of n=3 separate experiments.

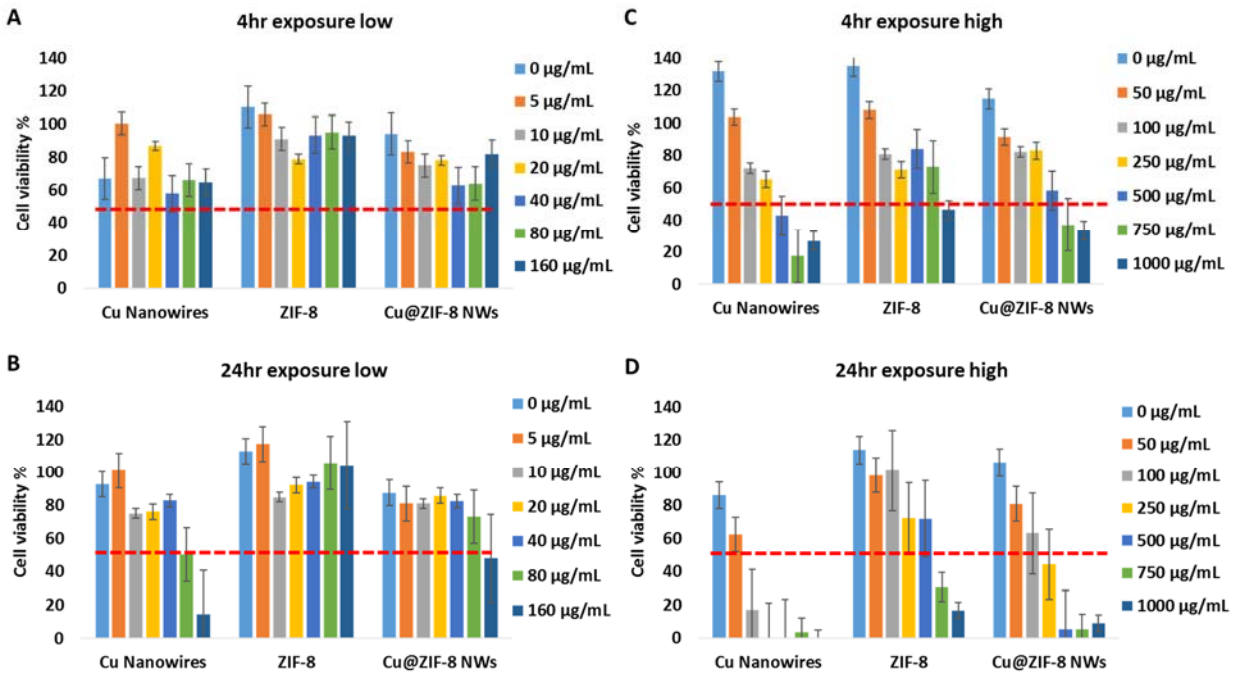


**Figure S11.** Effect of CuNWs, ZIF-8, and Cu@ZIF-8 NWs on viability of KB epithelial cells using the MTT assay after 4 h and 24 h exposure. Our results show that Cu@ZIF-8 shows no significant decrease in cell viability up to 80 µg/mL for low dose exposure and up to 100 µg/mL for high dose exposures. Data shown are mean ± SD of n=3 separate experiments.

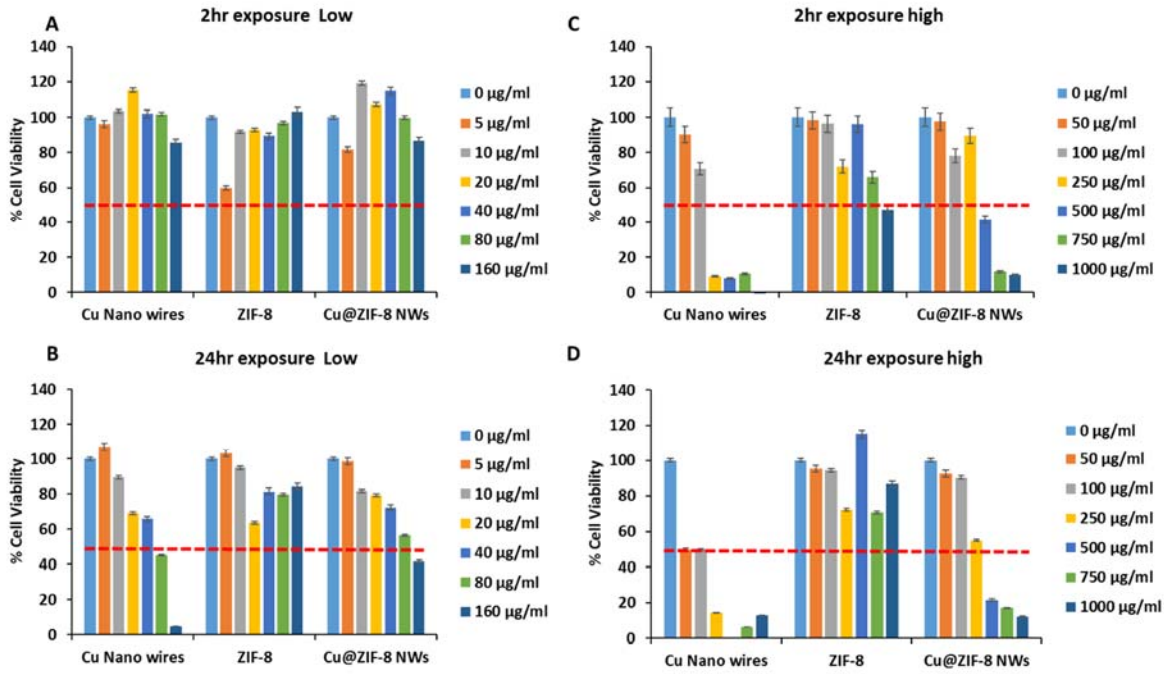


**Figure S12.** Effect of CuNWs, ZIF-8, and Cu@ZIF-8 NWs on viability of A549 adenocarcinomic human alveolar basal epithelial cells using the MTT assay after 2 h and 24 h exposure. Our results show that Cu@ZIF-8 shows no significant decrease in cell viability up to 80 µg/mL for low dose exposure and up to 250 µg/mL for high dose exposures. Data shown are mean ± SD of n=3 separate experiments.

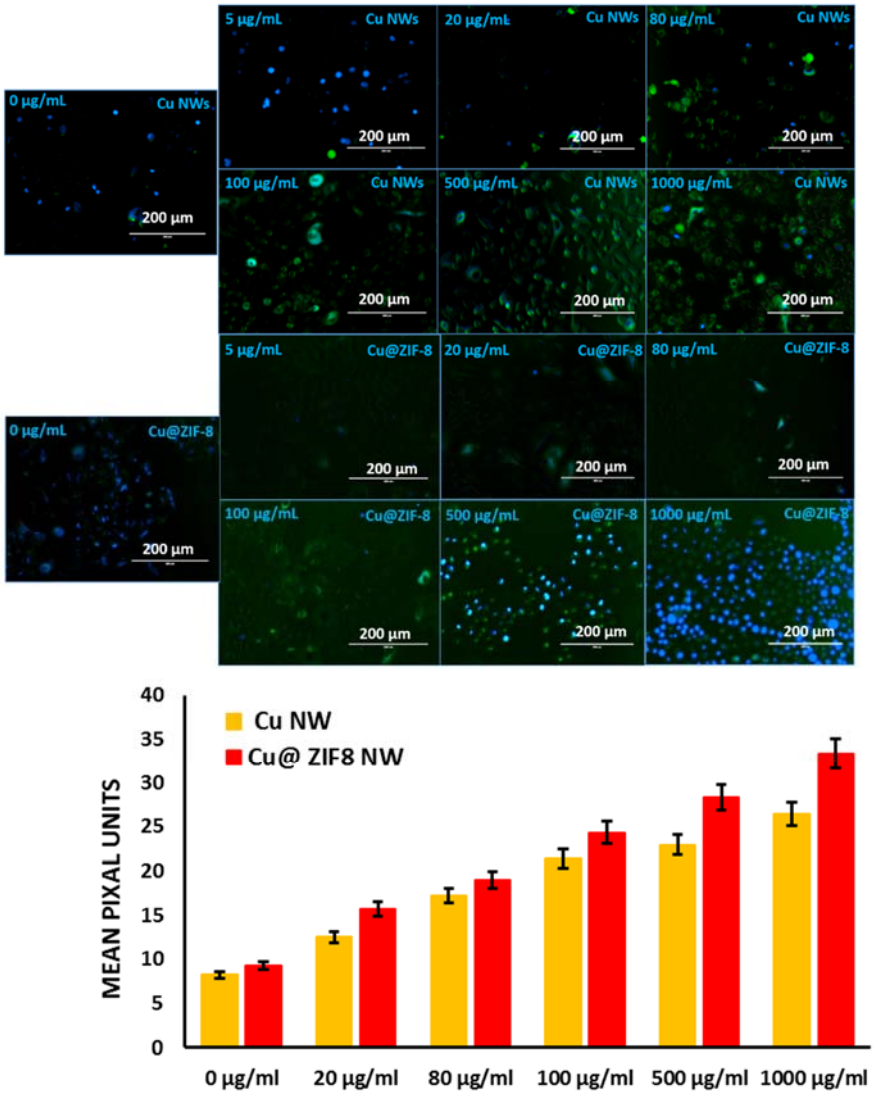


**Figure S13.** Determination of cellular ROS generation by fluorescence microscopic imaging of treated cells and spectrophotometric fluorescence intensity measurement which indicates the enhancement of ROS in cells treated with different concentrations of CuNWs and Cu@ZIF-8 (0, 20, 80, 100, 500 & 1000 µg/mL as labelled). Blue fluorescence is from DAPI staining of the cell nuclei; green fluorescence is from ROS-sensitive dye carboxy-H2DCFDA. The accompanying bar chart summarizes results of n=3 separate experiments in which the fluorescence signal intensity of ROS was quantified in pixel units using the Image J software.

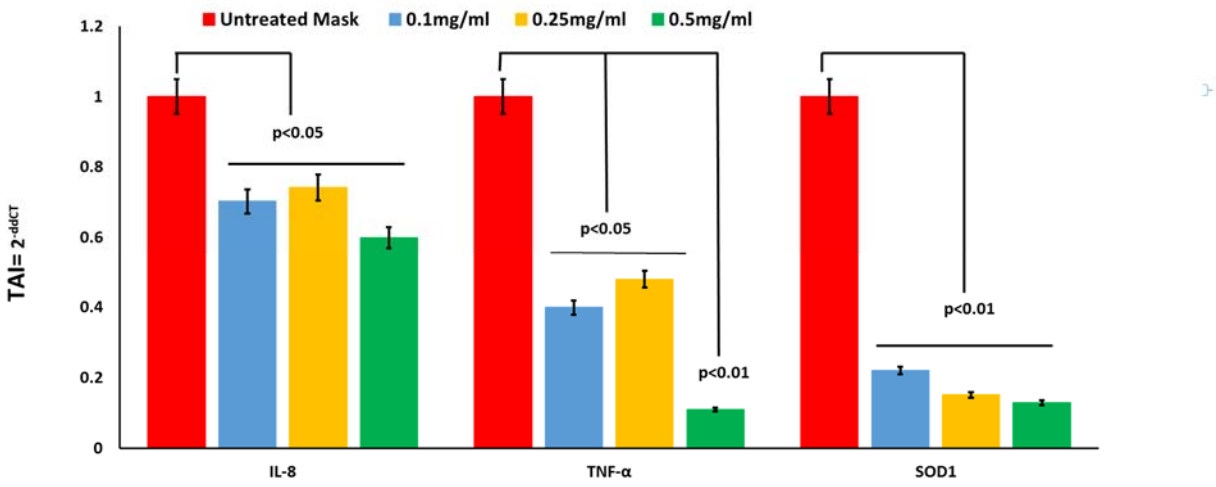


**Figure S14.** Effect of Cu@ZIF-8 on the gene expression levels of biomarkers of cellular oxidative stress and pro-inflammatory cytokines. A549 cells were treated with Cu@ZIF-8, and the gene expression levels of pro-inflammatory cytokines (IL-8, and TNF-α) and SOD1 were quantified by real time qPCR. Results are expressed as the mean ± SD of 3 separate experiments. Data is expressed as Transcript Accumulation Index (TAI) where $TAI=2^{-ddCT}$ calculated using the housekeeping gene β-actin as an internal assay control.

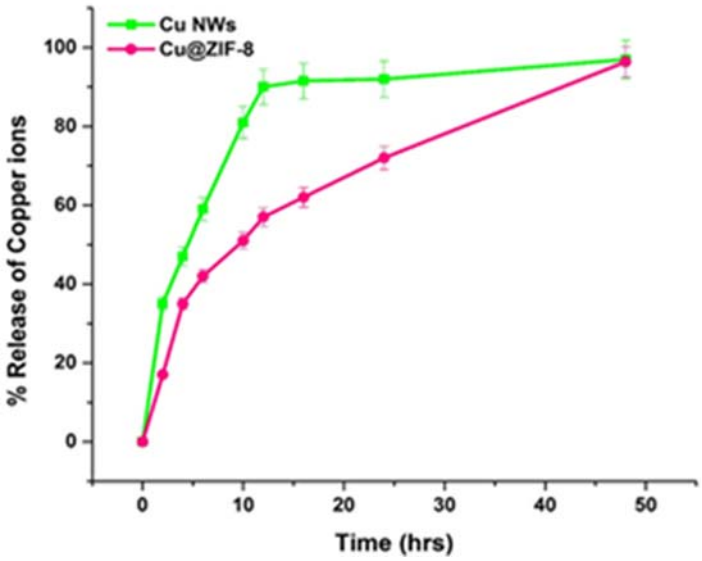


**Figure S15.** Release profile of copper ions from Cu NWs and Cu@ZIF-8 NWs in Brain Heart Infusion (BHI) media (n=3. $p<0.05$), with amount released after 48 h taken as 100%.

**(a)**

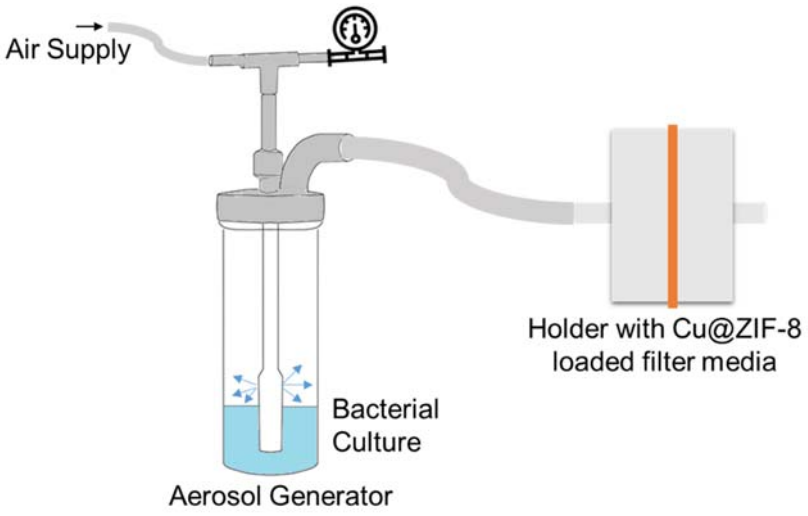


**(b)**

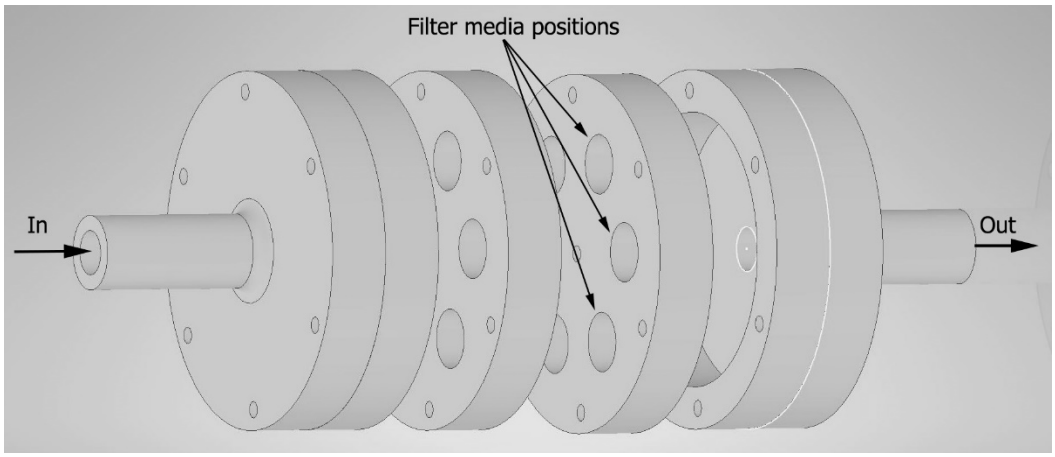


**Figure S16.** Schematic of bacterial aerosol-exposure test setup, as described in the manuscript. (a) overall setup, and (b) exploded view of 6-position filter media holder.

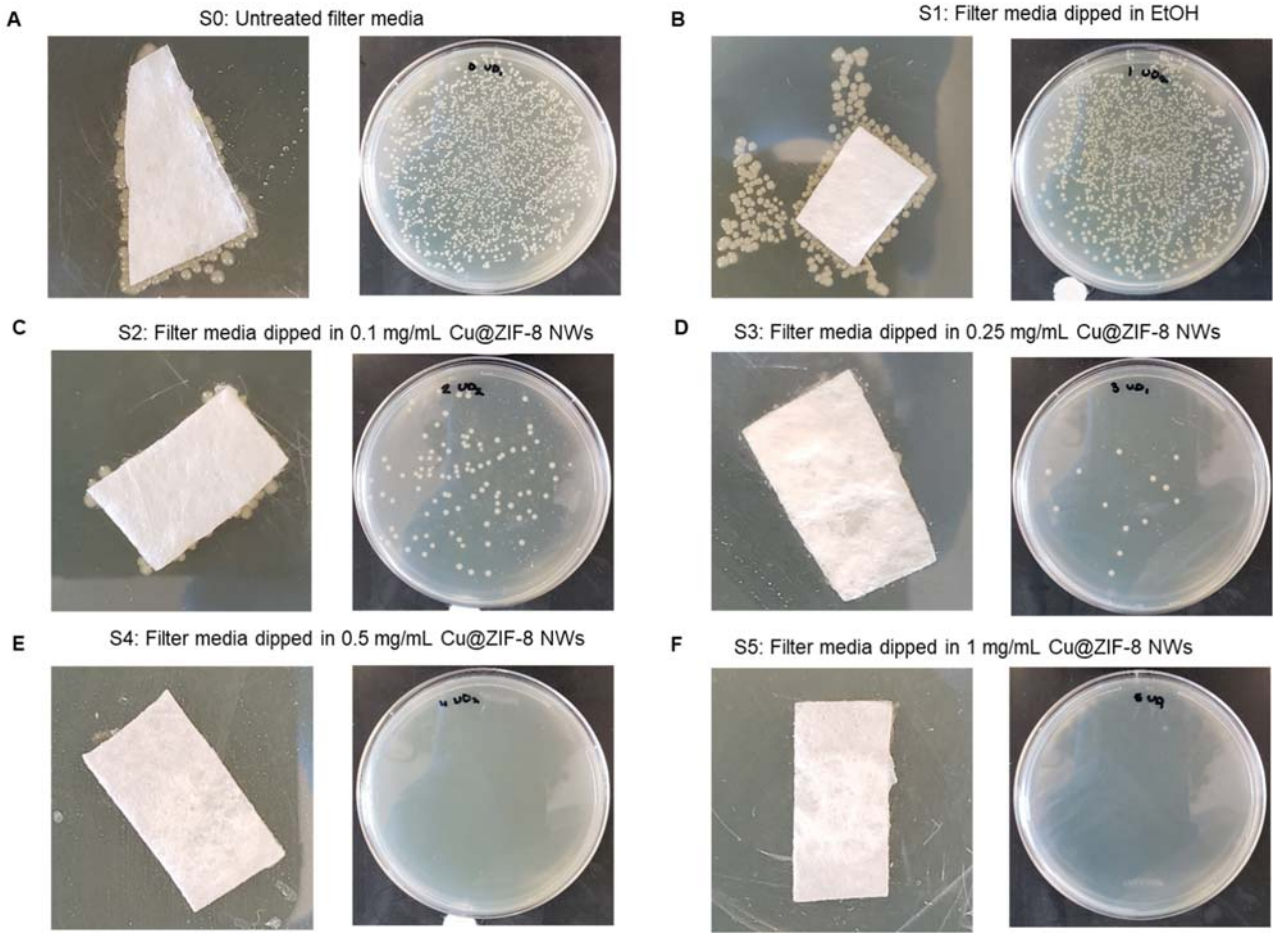


**Figure S17.** Antibacterial assays of untreated (S0), ethanol treated (S1), and Cu@ZIF-8 NW-functionalized filter media (S2-S5) and extracts from them (in saline) on agar plates. Photographs of Cu@ZIF-8 NWs functionalized filter media after exposure to bacteria-laden aerosols produced from *E. coli* suspensions for 30 min showing excellent bactericidal potential of Cu@ZIF-8 NWs. These are representative results of two experiments giving nearly identical results.